

## Ultrasonic Studies in Normal and Superconducting Thallium\*†

RAOUL WEIL‡ AND A. W. LAWSON

*Department of Physics, University of California, Riverside, California*

(Received 20 August 1965)

The velocity and attenuation of ultrasonic waves have been determined in thallium for the case  $ql < 1$ . The data are used to verify Pippard's semiclassical theory of the attenuation of sound by normal electrons. The elastic constants are given at 4.2 and 297°K. The value of the superconducting energy gap is determined for several directions of propagation and polarization of shear waves and found to be slightly anisotropic. A strain-amplitude dependence of the attenuation is found, which occurs after a minimum threshold is attained.

### I. INTRODUCTION

ULTRASONIC-attenuation studies of superconductors afford an opportunity to isolate the normal electronic component of the attenuation from all the other contributions. This is because electrons in the superconducting state do not contribute to the attenuation process below the gigacycle frequency range. Thus, by taking the difference between the normal and the superconducting attenuation, it is possible to calculate the electronic attenuation. Pippard<sup>1-5</sup> has developed phenomenological expressions for the ultrasonic attenuation of normal electrons as a function of the velocity of sound propagation, the frequency of the sound wave, the mean free path of the normal conduction electrons, the shape of the Fermi surface, and the density of the material. Thallium is a good material to test Pippard's theoretical results since (a) it becomes superconducting at a reasonably high temperature, (b) large single crystals of it are available, (c) its hexagonal structure<sup>6</sup> permits a variety of different modes of propagation along the different principal axes, and (d) both theoretical<sup>7-9</sup> and experimental<sup>10-12</sup> studies of the Fermi surface of thallium exist. Accordingly, measurements have been undertaken of ultrasonic attenuation as a function of frequency for five different directions of propagation—polarization.

Ultrasonic-velocity measurements lend themselves to the determination of the adiabatic elastic constants of a material.<sup>13</sup> From these, in turn, it is possible to infer the effect of lattice distortions on the Fermi surface.<sup>14,15</sup> Furthermore, the knowledge of the elastic constants of a material is of general interest. This is especially true in the case of hexagonal elements since from the various compilations consulted<sup>16-19</sup> it is apparent that Be, Cd, Co, Mg, Y, and Zn are the only elements of this structure whose elastic constants have been measured, and of these, only Y belongs to Group III. With these objectives in mind, the velocities of sound have been measured along the appropriate crystallographic directions at a frequency of 12 Mc/sec at room temperature and at 4.2°K.

Finally, ultrasonic attenuation can also be used as a tool to measure the superconducting energy gap in a material.<sup>20</sup> Using longitudinal waves, Saunders and Lawson<sup>21</sup> report an anisotropy in the gap for thallium. Since additional information about the anisotropy of the gap can be obtained from shear-wave attenuation measurements,<sup>22</sup> these were performed for three independent combinations of the propagation and polarization vectors. Detailed studies have been carried out at 60 Mc/sec. Additional measurements at other frequencies, in the range of 12 to 108 Mc/sec, have also been made to detect possible variations in the gap or its anisotropy.

In Sec. II the experimental details are given. In Sec. III the results of the measurements aimed at establishing the applicability of Pippard's equations are presented. In Sec. IV the elastic constants are investi-

\* This work was supported in part by a grant from the National Science Foundation.

† Based on a dissertation by R. B. Weil submitted in partial fulfillment of the requirements for a Ph.D.

‡ Present address: Monsanto Company, St. Louis, Missouri.

<sup>1</sup> A. B. Pippard, *Phil. Mag.* **46**, 1104 (1955).

<sup>2</sup> A. B. Pippard, *Rept. Progr. Phys.* **23**, 176 (1960).

<sup>3</sup> A. B. Pippard, *The Fermi Surface* (John Wiley & Sons, Inc., New York, 1960), p. 224.

<sup>4</sup> A. B. Pippard, *Proc. Roy. Soc. (London)* **257**, 165 (1960).

<sup>5</sup> A. B. Pippard, *Low-Temperature Physics* (Gordon and Breach, Science Publishers, Inc., New York, 1962), p. 110.

<sup>6</sup> R. W. G. Wyckoff, *Crystal Structures* (Interscience Publishers Inc., New York, 1948), Vol. 1.

<sup>7</sup> W. A. Harrison, *Phys. Rev.* **118**, 1190 (1960).

<sup>8</sup> P. Soven, *Phys. Rev.* **137**, A1706 (1965).

<sup>9</sup> P. Soven, *Phys. Rev.* **137**, A1717 (1965).

<sup>10</sup> J. A. Rayne, *Phys. Rev.* **131**, 653 (1963).

<sup>11</sup> N. E. Alekseevskii and Yu. P. Gaidukov, *Zh. Eksperim. i Teor. Fiz.* **36**, 447 (1959) [English transl.: *Soviet Phys.—JETP* **9**, 311 (1959)].

<sup>12</sup> N. E. Alekseevskii and Yu. P. Gaidukov, *Zh. Eksperim. i Teor. Fiz.* **43**, 2094 (1962) [English transl.: *Soviet Phys.—JETP* **16**, 1481 (1963)].

<sup>13</sup> W. P. Mason, *Physical Acoustics and the Properties of Solids* (D. Van Nostrand Company, Inc., Princeton, New Jersey, 1958), p. 371.

<sup>14</sup> R. S. Leigh, *Phil. Mag.* **42**, 139 (1951).

<sup>15</sup> J. R. Reitz and C. S. Smith, *Phys. Rev.* **104**, 1253 (1956).

<sup>16</sup> R. F. S. Hearmon, *Revs. Mod. Phys.* **18**, 409 (1946).

<sup>17</sup> H. B. Huntington, *Solid State Phys.* **7**, 213 (1958).

<sup>18</sup> *American Institute of Physics Handbook*, edited by D. E. Gray (McGraw-Hill Book Company, Inc., New York, 1963), 2nd ed., p. 2-53.

<sup>19</sup> W. P. Mason, *Piezoelectric Crystals and Their Application to Ultrasonics* (D. Van Nostrand Company, Inc., Princeton, New Jersey, 1950), p. 418.

<sup>20</sup> R. W. Morse, *Prog. Cryogenics* **1**, 219 (1959).

<sup>21</sup> G. A. Saunders and A. W. Lawson, *Phys. Rev.* **135**, A1161 (1964).

<sup>22</sup> J. R. Leibowitz, *Phys. Rev.* **136**, A22 (1964).

gated. In Sec. V the superconducting energy gap measurements are discussed. Lastly, in Sec. VI a summary of the results of this study and the pertinent conclusions are given.

## II. EXPERIMENTAL DETAILS

The samples were the same as those used by Saunders and Lawson.<sup>21</sup> They consisted of two cylinders: one (A) with its axis parallel to the [0001] direction and one (B) with its axis parallel to the [1010] direction. These samples were grown by a strain anneal technique from material in which only traces of impurities were spectroscopically detectable.<sup>23</sup> Despite the fact that the initial purity is better than 99.999%, from measurements which are described below, it is found that the mean free path in our samples is only about  $10^{-4}$  cm. We believe that oxygen may have been introduced to the samples in the vacuum premelting of the bars from which the crystals were grown.

Sample B was shortened by spark cutting yielding sample C to accommodate measurements for which the attenuation was very high. The remainder of sample B was cut to yield sample D whose axis was oriented at  $45^\circ$  to the C axis and the [1210] direction. Sample D was strained accidentally during the forming process but was only used for the determination of elastic constants. Sample E was a long thin cylinder cut from the remaining stock from which crystals A and B had been obtained. This sample was used in residual resistance measurements. The samples showed striations on the surface after spark cutting and etching, suggesting the presence of dislocations; however, reannealing the samples apparently had no effect on their attenuation.

Both sound-velocity and attenuation measurements were made using a double-ended pulse-echo technique.<sup>24</sup> Quartz transducers with a 12-Mc/sec fundamental frequency were attached to the ends of the thallium cylinders with Nonaq. The composite system was mounted in a suitable holder in a horizontal position directly in liquid helium. The ground return was through the sample. The samples were approximately  $\frac{3}{4}$  in. in diameter and the quartz transducers were  $\frac{1}{2}$  in. in diameter.

Provisions were made to measure the temperature from the helium vapor pressure and from the resistance of an Allen Bradley 0.1-W, 100- $\Omega$  carbon resistor, directly affixed to the sample. The temperature was lowered down to 1.2°K by pumping with a Welch Scientific Company type 1397 vacuum pump. The pressure was controlled by a manostat.

The various schemes used to determine the attenuation are illustrated in the block diagrams of Fig. 1.

<sup>23</sup> The analyses were kindly carried out by G. R. Bradford of the Citrus Experimental Station.

<sup>24</sup> W. P. Mason, *Physical Acoustics and the Properties of Solids* (D. Van Nostrand Company, Inc., Princeton, New Jersey, 1958), p. 101.

The most precise results were obtained with Scheme 2 as the attenuation only depended on passive electrical elements. For Schemes 1 and 4, calibration of the receiver is necessary. With reference to Fig. 1, the pulse generator is an Arenberg Ultrasonic Laboratory Model PG-6506. The buffer consists of two 1N67 diodes back to back. Attenuators A1 and A2 are respectively a Telonic and an Arenberg step attenuator. PPA is a variable precision piston attenuator which was part of a Cutler-Hammer, A1L Type 132 precision test receiver. The preamplifier is an Arenberg type PA620B unit and the wide-band amplifier is an Arenberg type WA-600-D modified to accommodate regulated filament supply. The oscilloscope is a Tektronic type 585 which has a variable calibrated trigger delay. A type-Z plug-in unit is used. The mixer is a Sage Laboratories model 2493 balanced mixer used in conjunction with a Hewlett-Packard 608-C signal generator.

The cryostat was mounted in an electromagnet and the field was determined by an Empire Scientific, Model 900, Hall probe gaussmeter. The field was provided to allow for magnetic quenching of the superconducting state.

## III. THE NORMAL ELECTRONIC ATTENUATION

Ultrasonic attenuation falls off in a superconductor which is cooled below its critical temperature  $T_c$ . This effect is caused<sup>25</sup> by the transition of electrons to the superconducting state. In this state the energy gap prevents them from participating in the attenuation process. At 0°K all the contribution of the electrons to attenuation will have vanished. Nevertheless a magnetic field, greater than a certain minimum peculiar to each superconductor, can destroy the superconducting state. We thus have a means to isolate from all other contributions the normal electronic attenuation  $\alpha_{en}$ ,

$$\alpha_{en} = \alpha_n(0) - \alpha_s(0), \quad (1)$$

where  $\alpha_n(0)$  and  $\alpha_s(0)$  are the attenuation, at 0°K, in the normal and superconducting states.

In our experiment with Tl, the lowest temperature reached is 1.2°K. As will be shown in Sec. V, only 95% of the electronic contribution to the attenuation is removed at this temperature. Our values of  $\alpha_{en}$  are correspondingly calculated from

$$\alpha_{en} = (1/0.95)[\alpha_n(1.2) - \alpha_s(1.2)]. \quad (2)$$

Pippard<sup>1-5</sup> has shown that, when  $ql < 1$ ,  $\alpha_{en}$  is given by

$$\alpha_{en} = \frac{\hbar q^2}{4\pi^3 M v_s} \int \int l D^2 dS, \quad (3)$$

where  $q$  and  $v_s$  are the sound wave vector and velocity,

<sup>25</sup> J. Bardeen, L. N. Cooper, and J. R. Schrieffer, *Phys. Rev.* **108**, 1175 (1957).

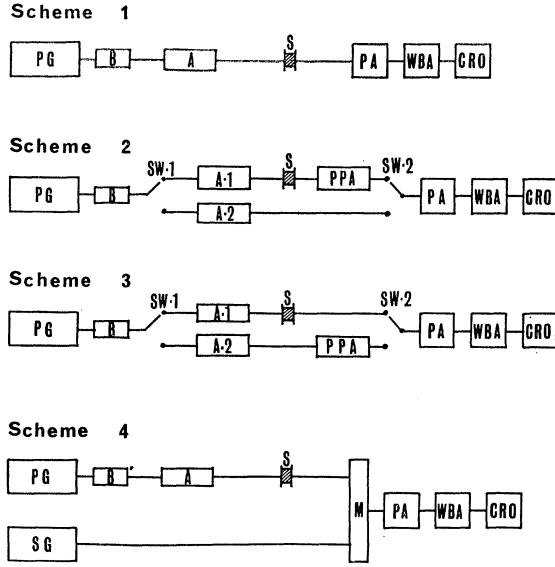


FIG. 1. Block diagram of electronic equipment used in various measuring schemes. Scheme 1 is for  $\omega \leq 60$  Mc/sec, schemes 2 and 3 for  $\omega \approx 60$  Mc/sec, and scheme 4 for  $\omega > 60$  Mc/sec. PG=pulse generator; B=buffer; SW-1, SW-2=coaxial switches; A, A-1, A-2=step attenuators; PPA=60 Mc/sec, precision piston attenuator; S=sample, PA=preamplifier, WBA=wide-band amplifier; GRO=cathode-ray oscilloscope; SG=signal generator; M=mixer.

respectively,  $M$  the density of the material,  $l$  the electronic mean free path,  $D$  a parameter dependent on the Fermi surface and  $dS$  an element of area on this surface. When  $ql \gg 1$  Pippard has shown that  $\alpha_{en}$  varies as  $\omega$ .

If  $q$  is expressed in terms of the sound frequency  $\omega$  and  $v_s$ , Eq. (3) can be written as

$$\alpha_{en} = \frac{\hbar\omega^2}{4\pi^3 M v_s^3} \iint l D^2 dS. \quad (4)$$

Using the measurements of  $\alpha_{en}$ , we have tested Pippard's relations and verified that indeed the frequency dependence goes as  $\omega^2$  and that the velocity dependence as  $v_s^{-3}$ .

Figure 2 shows a log-log plot of  $\alpha_{en}$  versus  $\omega$  for 5 different combinations of propagation and polarization directions. The straight lines are drawn with a slope of 2, showing that in most of the range  $\alpha_{en}$  is proportional to  $\omega^2$ . Since Morse<sup>20</sup> has demonstrated experimentally that the  $ql$  dependence of  $\alpha_{en}$  calculated by Pippard is obeyed closely, we interpret Fig. 2 to mean that  $ql < 1$  over most of the frequency range used.

Pippard<sup>5</sup> has shown that for a spherical Fermi surface Eq. (4) reduces to

$$\alpha_{en} = A (N m v \omega^2 / M v_s^3), \quad (5)$$

where  $N$  is the number of valence electrons per unit volume and  $m$  is the free electron mass. The constant  $A$  is  $4/15$  for longitudinal waves and is  $1/5$  for transverse waves.

TABLE I. Ultrasonic velocities for various propagation and polarization directions in Tl.  $\omega = 12$  Mc/sec,  $T = 297$  and  $4.2^\circ\text{K}$ .

Label	Direction of wave propagation	Direction of wave polarization	Sound velocity (cm/sec)	
			$T = 297^\circ\text{K}$	$T = 4.2^\circ\text{K}$
$v_{s1}$	[0001]	[0001]	$2.15 \times 10^5 \pm 0.5\%$	$2.25 \times 10^5 \pm 0.5\%$
$v_{s2}$	[1010]	[1010]	1.88	1.94
$v_{s3}$	[0001]	[1010]	0.780	0.864
$v_{s4}$	[1010]	[0001]	0.778	0.864
$v_{s5}$	[1010]	[1210]	0.474	0.529
$v_{s6}$	[121 3.2]	[121 3.2]	1.98	2.06
$v_{s7}$	[121 3.2]	[1010]	0.655	0.720
$v_{s7}$	Calculated <sup>a</sup>		0.645	$0.716 \pm 1.6\%$

$$^a v_{s7} = \left( \frac{c_{11} - c_{12} + 2c_{44}}{4M} \right)^{1/2}.$$

If then the free-electron model is applicable, and the  $v_s^{-3}$  dependence is correct, a plot of  $\log \gamma \alpha_{en}$  versus  $\log v_s$  should give a straight line of slope  $-3$ . Here  $\gamma = 1$  for longitudinal waves and  $\gamma = \frac{2}{3}$  for shear waves. Figure 3 is such a plot for thallium. The values of  $\alpha$  are taken from Fig. 2 at 20 Mc/sec. The corresponding values of  $v_s$  are taken from Table I ( $T = 4.2^\circ\text{K}$ ). The straight line in Fig. 3 is drawn with a slope of  $-3$ , and it is seen to fit three of the points within the experimental error. The point corresponding to  $q \parallel [1010]$ ,  $s \parallel [0001]$  and  $q \parallel [0001]$ ,  $s \parallel [1010]$  has a deviation which is not accountable by experimental error. It is not likely that the deviation could be caused by a misalignment of the crystals because the misplaced point corresponds to measurements made with two crystals aligned along the basal plane the  $c$  axis, respectively. Nevertheless,

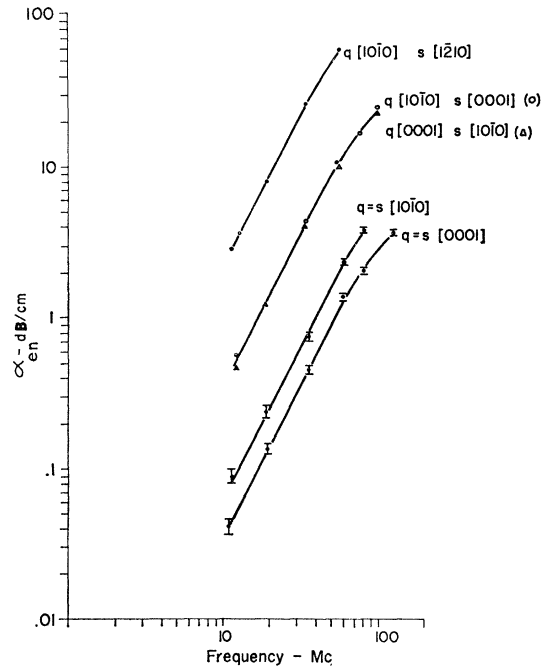


FIG. 2. Ultrasonic frequency dependence of normal electronic attenuation measured for different combinations of propagation, direction  $q$  and polarization direction  $s$ .

it is felt that Fig. 3 supports the  $v_s^{-3}$  dependence of  $\alpha_{en}$  derived by Pippard.

Pippard observes that serious errors can result from the use of a single relaxation time over a Fermi surface, especially if the surface is complicated as in Tl.<sup>8</sup> It is therefore remarkable that a good fit was obtained in Fig. 3 using a free-electron calculation to evaluate  $\iint l^2 D^2 dS$ .

An estimate of the mean free path can be obtained from the frequencies at which the  $\alpha_{en}$  pass from behavior characterized by  $ql < 1$  to that characterized by  $ql > 1$ . These frequencies can be obtained from Fig. 2 as those at which the straight lines start to bend. From these frequencies and from the velocities listed in Table I,  $q = \omega/v_s$  can be calculated, and from it  $l = 1/q$ . The results of these calculations give values of  $l$  varying between  $2 \times 10^{-4}$  cm and  $5 \times 10^{-4}$  cm.

Equation (5) can also be solved for  $l$ . The values of  $\alpha_{en}$  (with  $\gamma = 1$ ) and  $v_s$  are read from Fig. 3 as 1.68 dB/cm = 0.386 nepers/cm at  $v_s = 10^5$  cm/sec,  $\omega$  is  $2\pi \times 20 \times 10^6$  rad/sec, and the rest of the parameters are taken from the free-electron model. The result of this calculation yields  $l = 0.67 \times 10^{-4}$  cm, in order of magnitude agreement with the previous calculations.

These results seem quite reasonable when compared to the residual resistance ratio  $R_{300^\circ}/R_{4.2^\circ}$  of  $10^3$  found in sample E. However, it should be noted that the mean free path in our samples is about 1000 times shorter than that found by Rayne, namely  $1.5 \times 10^{-1}$  cm, for samples presumably prepared in a similar fashion. As already noted, we believe this discrepancy is accounted for by the inadvertent introduction of oxygen in the premelting process.

#### IV. ELASTIC CONSTANTS

Owing to the hexagonal symmetry of thallium, 16 of the 21 independent elastic constants may be eliminated. Five independent elastic constants comprise the stiffness matrix:

$$C_{rs} = \begin{pmatrix} C_{11} & C_{12} & C_{13} & 0 & 0 & 0 \\ C_{12} & C_{11} & C_{13} & 0 & 0 & 0 \\ C_{13} & C_{13} & C_{33} & 0 & 0 & 0 \\ 0 & 0 & 0 & C_{44} & 0 & 0 \\ 0 & 0 & 0 & 0 & C_{44} & 0 \\ 0 & 0 & 0 & 0 & 0 & \frac{1}{2}(C_{11} - C_{12}) \end{pmatrix}. \quad (6)$$

The compliance matrix  $S_{sr}$  is similar except  $S_{66} = 2(S_{11} - S_{12})$ . The relations between  $S_{sr}$  and  $C_{rs}$  are given by Voigt.<sup>26</sup> The elastic constants can be calculated from the ultrasonic velocities in the different crystallographic directions. Appropriate formulas are given by Mason.<sup>13</sup> In general  $C_{11}$ ,  $C_{33}$ ,  $C_{44}$ , and  $C_{12}$  may be determined by measuring the longitudinal and shear velocities in each of two principal crystallographic

<sup>26</sup> W. Voigt, *Lehrbuch der Kristallphysik* (B. G. Teubner, Leipzig, 1928), p. 747.

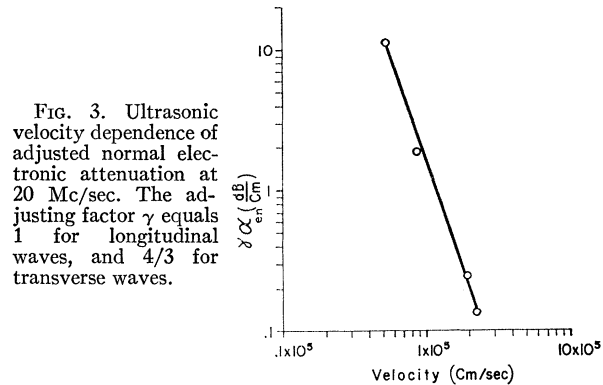


FIG. 3. Ultrasonic velocity dependence of adjusted normal electronic attenuation at 20 Mc/sec. The adjusting factor  $\gamma$  equals 1 for longitudinal waves, and  $4/3$  for transverse waves.

directions. To obtain  $C_{13}$  one must use some non-principal crystallographic direction such as the axis of sample D.

Table I lists the sound velocities calculated from measurements at room temperature ( $297^\circ\text{K}$ ) and  $4.2^\circ\text{K}$ . The time intervals between pulses were all measured at frequencies in the range of 10.5 to 13.0 Mc/sec where at least four pulses were visible for all crystallographic directions. In each particular case, the frequency was adjusted to give the set of pulses of best shape. The lengths of the samples at  $4.2^\circ\text{K}$  were calculated from the room-temperature measurements by applying expansion coefficients calculated from Barrett's<sup>27</sup> x-ray diffraction measurements at  $23^\circ\text{C}$  and  $5^\circ\text{K}$ . No correction was made for the transducers' thickness because pulse transit time measurements made on samples of different lengths showed that, within the precision of the experiment, the time was proportional to the length.

Two internal checks are available for the velocities. One check is the comparison of  $v_{s3}$  and  $v_{s4}$  which should be,<sup>13</sup> and are, the same. The other check is the comparison of the measured and calculated values of  $v_{s7}$ . These values are shown to agree in Table I.

Table II presents the elastic constants for thallium both at room temperature and  $4.2^\circ\text{K}$ . The table also lists the equations used to calculate the constants. The values used for the density at room temperature and  $4.2^\circ\text{K}$  are 11.89 and 12.10 g/cm<sup>3</sup>, respectively. These values have been calculated from Barrett's x-ray measurements.

The probable errors quoted in Tables I and II are rms deviations. These are calculated from the estimated errors in the length and time measurements.

We turn now to the evaluation of the Debye temperature  $\Theta_D$  which is related to the velocity of sound  $v_s$  by the equation,

$$\Theta_D = (\hbar/k_B)(6\pi^2N)^{1/3}(v_s)_{av}, \quad (7)$$

where  $\hbar$  is Planck's constant,  $k_B$  is the Boltzmann constant and  $N$  is Avogadro's number.

<sup>27</sup> C. S. Barrett, *Phys. Rev.* **110**, 1071 (1958).

TABLE II. Adiabatic elastic constants of Tl at 297 and 4.2°K.

$c_{rs}$	Formula	Stiffness (dyn/cm <sup>2</sup> )	
		$T=297^\circ\text{K}$	$T=4.2^\circ\text{K}$
$c_{11}$	$v_s^2 M$	$4.19 \times 10^{11} \pm 1\%$	$4.53 \times 10^{11} \pm 1\%$
$c_{33}$	$v_s^2 M$	5.49 $\pm 1\%$	6.11 $\pm 1\%$
$c_{44}$	$v_s^2 M$	0.720 $\pm 1\%$	0.903 $\pm 1\%$
$c_{12}$	$c_{11} - 2v_s^2 M$	3.66 $\pm 1.2\%$	3.86 $\pm 1.2\%$
$c_{13}$	a	2.99 $\pm 3.6\%$	2.92 $\pm 3.6\%$

$s_{rs}$	Formula	Compliance (cm <sup>2</sup> /dyn)	
		$T=297^\circ\text{K}$	$T=4.2^\circ\text{K}$
$s_{11}$	$\frac{1}{2} \left[ c_{33} s' + \frac{1}{c_{11} - c_{12}} \right]^b$	$10.44 \times 10^{-12} \pm 10\%$	$8.27 \times 10^{-12} \pm 8\%$
$s_{33}$	$(c_{11} + c_1) s'^b$	3.11 $\pm 5\%$	2.45 $\pm 3\%$
$s_{44}$	$\frac{1}{c_{44}}$	13.9 $\pm 1\%$	11.1 $\pm 1\%$
$s_{12}$	$\frac{1}{2} \left[ c_{33} s' - \frac{1}{c_{11} - c_{12}} \right]^b$	-8.27 $\pm 13\%$	-6.49 $\pm 10\%$
$s_{13}$	$-c_{13} s'^b$	-1.16 $\pm 10\%$	-0.854 $\pm 8\%$

$$^a c_{13} = \left\{ \left[ 2Mv_s^2 - \left( \frac{c_{11} + c_{33} + 2c_{44}}{2} \right) \right]^2 - \left( \frac{c_{11} - c_{33}}{2} \right)^2 \right\}^{1/2}.$$

$$^b s' = [(c_{11} + c_1)c_{33} - 2(c_{13})^2]^{-1}.$$

The problem is to compute  $(v_s)_{\text{av}}$ . We have used the procedure developed by Anderson.<sup>28</sup> In this manner, we find  $\Theta_D$  to be 83.2°K which compares favorably with the value of 85°K obtained by van der Hoeven and Keesom<sup>29</sup> from specific-heat measurements.

The compressibility which was measured many years ago by Richards and White<sup>30</sup> affords another possible check on the elastic constants. The adiabatic compressibility  $\beta$  may be calculated from our compliance coefficients by the relation,

$$\beta = 2S_{11} + S_{33} + 2S_{12} + 4S_{13}. \quad (8)$$

The resultant value is  $2.80 \times 10^{-12}$  cm<sup>2</sup>/dyn  $\pm 1.5\%$ . The corresponding isothermal value is  $2.96 \times 10^{-12}$  cm<sup>2</sup>/dyn  $\pm 1.5\%$ . Equation (8) assumes that the pressure is uniformly transmitted and according to Hill<sup>31</sup> represents the upper limit for the compressibility of a randomly oriented polycrystalline sample. The lower limit is set by assuming that the strain is uniformly distributed. In this case, according to Hill the compressibility  $\beta_v$  is given by Voigt's equation

$$\beta_v = [2C_{11} + C_{33} + 2C_{12} + 4C_{13}]^{-1}. \quad (9)$$

The isothermal compressibility calculated from Eq. (9) is  $2.87 \times 10^{-12}$  cm<sup>2</sup>/dyn  $\pm 1.5\%$ . Richards and White's value of  $2.83 \times 10^{-12}$  cm<sup>2</sup>/dyn is slightly outside the extreme limits calculated by us but the agreement must nevertheless be considered good.

The elastic constants are also of interest in connection with the superconductivity of thallium in which it is

reported<sup>32</sup> that  $\partial H_c / \partial P > 0$ , where  $H_c$  is the critical field and  $P$  is the pressure. In other superconductors, the inequality is of the opposite sense. Cody<sup>33</sup> has found that in thallium  $\partial H_c / \partial P_1$ , where  $P_1$  is the stress perpendicular to the  $c$  axis, is also positive. He suggests that these anomalies could be accounted for if the elastic constants of Tl have an anisotropy such that

$$|S_{13}| > (S_{11} + S_{12}). \quad (10)$$

Using the elastic constants measured at 4.2°K, we find that

$$-S_{13} - S_{11} - S_{12} = -0.93 \pm 0.01 \times 10^{-12} \text{ cm}^2/\text{dyn}. \quad (11)$$

From Eq. (10) one would expect Eq. (11) to yield a positive value. Since this is not the case, the anomalies in Tl must be ascribed to another origin than the elastic constants.

A theoretical calculation of the elastic constants using Huntington's formula,<sup>17</sup> which only takes into account the electrostatic energy needed to assemble the lattice, yields stiffness constants of the order of 5 times larger than the experimental values. This is undoubtedly due to the complicated band structure of Tl as can be surmised from Reitz's<sup>15</sup> calculations on Mg. This author adapted to the hexagonal symmetry a method of calculation devised by Leigh<sup>14</sup> for Al. This method takes into account the effect of the Fermi sea on the elastic constants. We suggest that a similar calculation carried out for Tl would bring the theoretical and experimental stiffness constants into agreement.

It thus seems that while the complicated Fermi surface of Tl does not severely affect  $\int \int \int D^2 dS$  in Eq. (3), the band structure, through its effect on  $v_s$ , plays a substantial role in determining  $\alpha_{en}$ .

## V. STUDIES IN THE SUPERCONDUCTING STATE

Levy,<sup>34</sup> using the Boltzmann transport equation to determine the dependence of shear wave attenuation on the superconducting energy gap  $\Delta(T)$ , has shown that the ratio of the attenuation  $\alpha_{es}$  of the superconducting electrons to that of the normal electrons  $\alpha_{en}$  is given by

$$\frac{\alpha_{es}}{\alpha_{en}} = 2 \left\{ \exp \left[ \frac{\Delta(T)}{k_B T} \right] + 1 \right\}^{-1}. \quad (12)$$

This equation, which is valid for  $ql < 1$ , is identical to that derived by Bardeen, Cooper, and Schrieffer<sup>25</sup> for longitudinal waves in the case  $ql \gg 1$  and shown by Tsuneto<sup>35</sup> to be valid in the latter case for  $0 < ql < \infty$ . Equation (12) is derived for an isotropic model but

<sup>28</sup> O. L. Anderson, J. Phys. Chem. Solids **24**, 909 (1963).

<sup>29</sup> B. J. C. van der Hoeven, Jr., and P. H. Keesom, Phys. Rev. **135**, A631 (1964).

<sup>30</sup> T. W. Richards and J. D. White, J. Am. Chem. Soc. **50**, 3290 (1928).

<sup>31</sup> R. Hill, Proc. Phys. Soc. (London) **A65**, 349 (1952).

<sup>32</sup> M. D. Fiske, J. Phys. Chem. Solids **2**, 191 (1957).

<sup>33</sup> G. D. Cody, Phys. Rev. **111**, 1078 (1958).

<sup>34</sup> M. Levy, Phys. Rev. **131**, 1497 (1963).

<sup>35</sup> T. Tsuneto, Phys. Rev. **121**, 402 (1961).

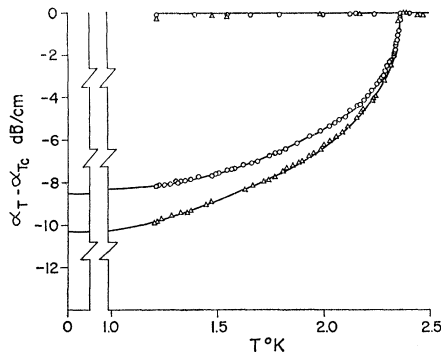


Fig. 4. Temperature dependence of ultrasonic attenuation.  $q \parallel [10\bar{1}0]$ ,  $s \parallel [0001]$ ,  $\omega = 58.1$  Mc/sec. Upper straight line is for specimen in the normal state. Lower curves are for superconducting state measurements. The voltage on the transducers are 1.8 and 79 V, respectively for points marked  $\circ$  and  $\Delta$ .

nevertheless, following common practice,<sup>21,36-39</sup> we shall use this equation to analyze the data even when the gap is anisotropic.

The experiments germane to this section consist of measurements of attenuation as a function of temperature, in both the normal and superconducting states. The results of these measurements have been plotted in a manner illustrated by Fig. 4. The reference level is taken as the attenuation at the transition temperature.

It is observed in Fig. 4 that  $\alpha_n$ , the attenuation in the normal state, is independent of temperature. Two curves are presented for  $\alpha_s$ , the attenuation in the superconducting state. The upper curve results when the strain amplitude of the sound pulse is large enough to cause a new attenuation mechanism to become effective. The results of a study of the strain amplitude effect are given in a later part of this section.

It is observed that  $\alpha_s$  shows no discontinuous drop at the transition temperature. Such a drop seems to be characteristic for the attenuation of shear waves when  $ql \gg 1$ ,<sup>20,40-42</sup> and is absent when  $ql < 1$ .<sup>36</sup> This characteristic of the  $\alpha_s$  curves is consistent with the other observations which indicate  $ql < 1$  for our measurements.

By use of Eq. (12) it is possible to calculate theoretical curves of  $\alpha_{es}/\alpha_{en}$  versus  $T/T_c$  for various values of the superconducting energy gap. To obtain these curves, one lets

$$\Delta = Ak_B T_c, \quad (13)$$

<sup>36</sup> M. Levy, R. Kagiwada, and I. Rudnick, Phys. Rev. **132**, 2039 (1963).

<sup>37</sup> R. W. Morse, T. Olsen, and J. D. Gavenda, Phys. Rev. Letters **3**, 15 (1959).

<sup>38</sup> P. A. Bezuglyi, A. A. Galkin and A. P. Korolyuk, Zh. Eksperim. i Teor. Fiz. **39**, 7 (1960) and **39**, 1163 (1960) [English transl.: Soviet Phys.—JETP **12**, 4 (1961) and **12**, 810 (1961)].

<sup>39</sup> E. R. Dobbs and J. M. Perz, Rev. Mod. Phys. **36**, 257 (1964).

<sup>40</sup> R. David, H. R. van der Laan, and N. J. Poulis, Physica **29**, 357 (1963).

<sup>41</sup> J. R. Leibowitz, Phys. Rev. **133**, A84 (1964).

<sup>42</sup> L. T. Claiborne, Jr., and R. W. Morse, Phys. Rev. **136**, A893 (1964).

where  $\Delta$  is the limiting gap at 0°K and  $A = 1.76$  in the BCS theory. If

$$\Gamma = \Delta(T)/\Delta, \quad (14)$$

Eq. (12) becomes

$$\frac{\alpha_{es}}{\alpha_{en}} = 2 \left\{ \exp \left[ \frac{A\Gamma T_c}{T} \right] + 1 \right\}^{-1}. \quad (15)$$

Muhlschlegel<sup>43</sup> has tabulated  $\Gamma$  in terms of  $T/T_c$  from the BCS theory. Using his data, a family of  $\alpha_{es}/\alpha_{en}$  versus  $T/T_c$  curves is obtained from Eq. (15) by letting  $A$  vary as a parameter. Therefore, while the BCS form for the temperature dependence of the gap is assumed, the gap at 0°K (characterized by  $A$ ) is allowed to take values different from the BCS prediction.

The experimental values of  $\alpha_{es}/\alpha_{en}$  are obtained from plots illustrated by Fig. 4. Since it is found in our experiment that  $\alpha_n$  is constant over the temperature range considered, we assume that the nonelectronic attenuation,  $\alpha_r$ , is also constant. Equation (12) states that  $\alpha_{es} = 0$  at  $T = 0$ ; therefore,  $\alpha_s(0) = \alpha_r$ . A first approximation to  $\alpha_s(0)$  is found by graphical extrapolation of the  $\alpha_s$  curve. Next,  $\alpha_{en}$  and  $\alpha_{es}$  are obtained by subtracting  $\alpha_r$  from  $\alpha_n$  and  $\alpha_s$ , respectively. Then  $\alpha_{es}/\alpha_{en}$  is calculated and plotted versus  $T/T_c$ . The plot is compared to the theoretical family of curves. If a good fit is not obtained with one of the theoretical curves, the extrapolated value of  $\alpha_s(0)$  is adjusted, and the procedure is repeated. Finally, the gap is obtained from the

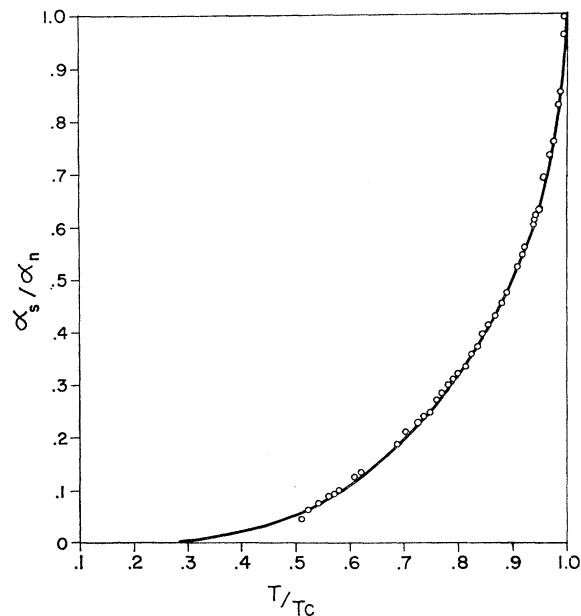


Fig. 5. Normalized attenuation as a function of reduced temperature  $q \parallel [10\bar{1}0]$ ,  $s \parallel [0001]$ ,  $\omega = 58.1$  Mc/sec, transducer excitation = 1.8 V. Solid line is theoretical curve corresponding to  $2\Delta = 3.75k_B T_c$ .

<sup>43</sup> B. Muhlschlegel, Z. Physik **155**, 313 (1959).

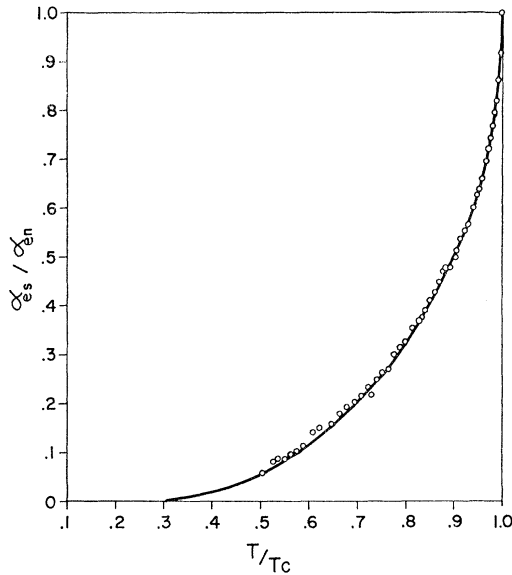


FIG. 6. Normalized attenuation as a function of reduced temperature  $q||[0001]$ ,  $s||[10\bar{1}0]$ ,  $\omega=58.2$  Mc/sec, transducer excitation=6 V. Solid line is theoretical curve corresponding to  $2\Delta=3.70k_B T_c$ .

value of  $A$  corresponding to the theoretical curve which matches the experimental data. It is estimated that this method gives a unique value for  $A$ , within  $\pm 0.05$ .

Shear-wave attenuation measurements have been performed for three  $\bar{q}$ - $\bar{s}$  combinations. The results are shown in the  $\alpha_{es}/\alpha_{en}$  versus  $T/T_c$  plots of Figs. 5, 6, and 7. These figures are for data taken at frequencies close to 60 Mc/sec, where the best accuracy in attenuation measurement is possible. Experiments at other frequencies, in the range from 12 to 108 Mc/sec, have also been performed. No frequency dependence of  $\alpha_{es}/\alpha_{en}$  has been observed. In all cases at the lowest temperature reached,  $\alpha_{es}/\alpha_{en}$  is 0.05; this observation is used in Eq. (2).

In Table III the results obtained for the superconducting energy gap of Tl are summarized, along with those reported by Saunders and Lawson.<sup>21</sup> A true comparison between Saunders and Lawson's values and ours is not feasible. Their extrapolation method to obtain  $\alpha_s(0)$  gives the  $BCS\Delta(T)/\Delta$  dependence only when  $T/T_c < 0.5$ . As the minimum temperature reached

TABLE III. Superconducting energy gap measured along different principal axes with transverse and longitudinal waves in thallium.

Material	Source	Propagation direction	Polarization direction	Energy gap ( $2\Delta k_B T_c$ )
Tl	Fig. 9	$[0001]$	$[10\bar{1}0]$	$3.7 \pm 0.1$
Tl	Fig. 8	$[10\bar{1}0]$	$[0001]$	$3.75 \pm 0.1$
Tl	Fig. 10	$[10\bar{1}0]$	$[1\bar{2}10]$	$3.9 \pm 0.1$
Tl	Ref. 21	$[0001]$	$[0001]$	$3.76 \pm 0.03$
Tl	Ref. 21	$[10\bar{1}0]$	$[10\bar{1}0]$	$4.10 \pm 0.03$
Tl	Ref. 21	$[1\bar{2}10]$	$[1\bar{2}10]$	$4.00 \pm 0.10$

in their experiment corresponds to  $T/T_c \approx 0.5$ , this extrapolation procedure yields a smaller gap than our procedure. On the other hand, from the shape of their curves of  $\alpha_{es}/\alpha_{en}$ , we surmise that they used strain amplitudes which were large enough to affect their gap measurement. It will be shown later that large strain amplitudes yield a gap value that is larger than the true gap. These two effects introduce discrepancies of opposite sign and therefore probably tend to cancel out.

During the course of the experiments to measure the energy gap, discrepancies have appeared in the  $\alpha$ -versus- $T$  curves. The source of the discrepancies has been traced to a dependence of attenuation on the strain amplitude, i.e., the voltage applied to the transmitting transducer. This dependence is illustrated by the two  $\alpha_s$  curves presented in Fig. 4. The upper curve is for a large voltage and Fig. 8 gives  $\alpha_{es}/\alpha_{en}$  versus  $T/T_c$  obtained from it. Except for the strain amplitude, Figs. 5 and 8 correspond to measurements taken under similar conditions; yet, these figures yield gaps of  $2\Delta=3.75k_B T_c$  and  $4.0k_B T_c$ , respectively. In order to interpret these observations, we have made a study of the strain-amplitude effect on the attenuation.

This study is limited to observations at 60 Mc/sec using reannealed sample C and the same  $\bar{q}$ - $\bar{s}$  as for Figs. 5 and 8. Scheme 2 of Fig. 1 has been used for attenuation measurement at and above 5-V excitation voltage and Scheme 3 for measurements below 5 V.

Figure 9 presents measurements of attenuation as a function of voltage amplitude on the transducer, at fixed temperatures. The various voltages on the transducer are obtained by varying attenuator A-1. To account for mismatch effects, the actual voltages have

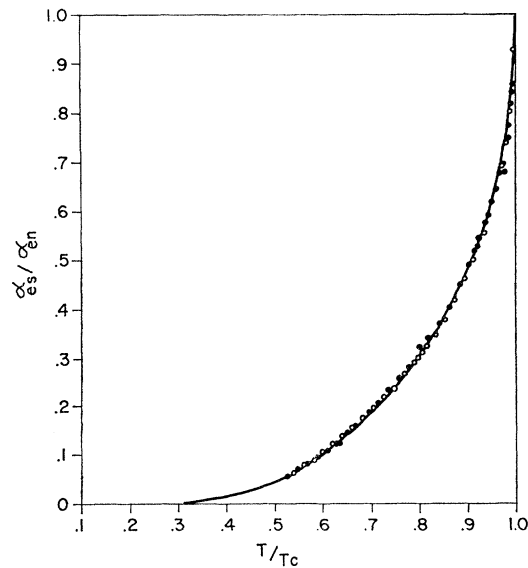


FIG. 7. Normalized attenuation as a function of reduced temperature  $q||[10\bar{1}0]$ ,  $s||[1\bar{2}10]$ ,  $\omega=58.4$  Mc/sec, transducer excitation=15 V. Solid line is theoretical curve corresponding to  $2\Delta=3.90k_B T_c$ . Data taken going down in temperature  $\bullet$  and going up in temperature  $\circ$ .

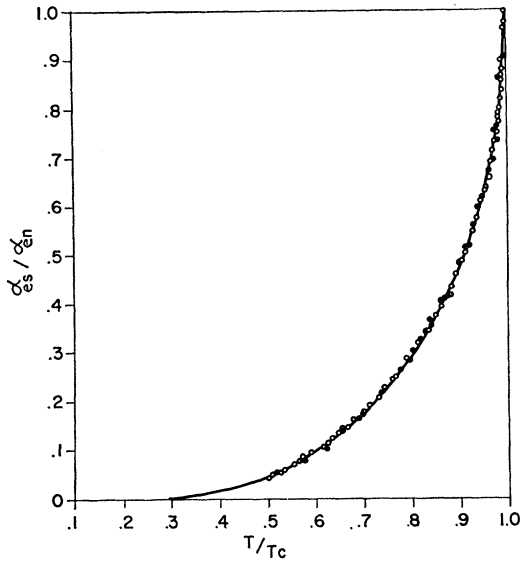


FIG. 8. Normalized attenuation as a function of reduced temperature.  $q \parallel [10\bar{1}0]$ ,  $s \parallel [0001]$ ,  $\omega = 58.1$  Mc/sec, transducer excitation = 79 V. Solid line is theoretical curve corresponding to  $2\Delta = 4.0k_B T_c$ . Data taken going down in temperature  $\circ$  and going up in temperature  $\bullet$ .

been measured at the transducer instead of being calculated from the nominal attenuation settings of A-1.  $\alpha_s$  and  $\alpha_n$  are determined from the attenuation in PPA and in A-1. During the experiment both the pulse generator output and the pulse height at the oscilloscope are maintained constant, therefore,

$$\alpha_n = \text{constant} - \alpha_{A-1} - \alpha_{PPA}. \quad (16)$$

A similar equation obtains for  $\alpha_s$ . The constant has been arbitrarily chosen at 36.00 dB. Thus only the relative values of  $\alpha_s$  and  $\alpha_n$  are meaningful in Fig. 9. On the other hand, the absolute values of  $\alpha_s - \alpha_n$  are significant because the constant subtracts out.

Figure 9 shows that a strain-amplitude-dependent attenuation mechanism becomes effective when the voltage on the transmitting transducer is greater than 50 V. Below this level,  $\alpha_s - \alpha_n$  is constant and the superconducting energy gaps calculated from this variable can be assumed independent of the strain-amplitude effect.

It is also evident from Fig. 9 that the strain-amplitude effect is more pronounced in the superconducting than in the normal state. As a matter of fact, the slope of  $\alpha_s$  is double the slope of  $\alpha_n$ . Consequently the slopes of  $\alpha_s - \alpha_n$  equals the slope of  $\alpha_n$ . We observe further that the strain-amplitude effect in  $\alpha_n$  is operative both above and below  $T_c$ . It is unlikely that the strain-amplitude effect is caused by changes in the bond attenuation, as it is improbable that such changes would be different in the normal and superconducting states. As for the effect on the elastic constants, no measurable strain-

amplitude dependence has been found in  $v_s$ , either in the normal or the superconducting states.

Strain-amplitude effects on ultrasonic attenuation have recently been found in Pb by Love *et al.*,<sup>44,45</sup> and by Tittmann and Bömmel.<sup>46</sup> The effect of strain-amplitude on  $\alpha_s$  versus  $T$  and on  $\Delta$  reported for Pb are the same as those we have found for Tl. On the other hand, none of the experiments on Pb reveal a significant strain-amplitude dependence of  $\alpha_n$ . It may be that this effect in normal Pb is masked by other mechanisms since in this metal  $\alpha_n$  is a strongly varying function of temperature at and below  $T_c$ . In Tl and other superconductors<sup>47,48</sup>  $\alpha_n$  does not vary appreciably in this temperature range. Another difference between the strain-amplitude effect in Tl and in Pb is that in the latter case apparently no threshold has been found below which the strain-amplitude effect is unobservable.

Tittman and Bömmel<sup>46</sup> suggest that an explanation of the strain-amplitude effect might be found within the frame of the Granato-Lücke<sup>49,50</sup> theory. This theory finds a strain-amplitude dependence in the attenuation produced by dislocations in the crystal structure. The mechanism proposed by Granato and Lücke assumes that dislocations are pinned by impurities which are separated by an average distance  $L_c$ . They also postulate the existence of a dislocation network in which the average distance between nodes is  $L_n$  where  $L_n > L_c$ . As long as the strain applied to the specimen is small, the dislocations are pinned at the impurities and the stress-strain relation is Hookean. When the strain is large, the dislocations break away from the impurity

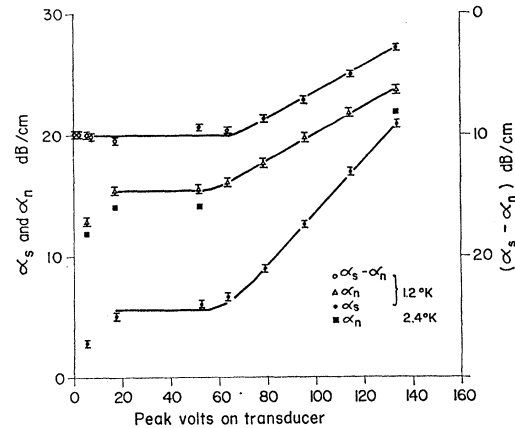


FIG. 9. Attenuation in the normal and superconducting states and their difference as a function of transducer excitation voltage.  $q \parallel [10\bar{1}0]$ ,  $s \parallel [0001]$ ,  $\omega = 58.1$  Mc/sec.

<sup>44</sup> R. E. Love and R. W. Shaw, *Rev. Mod. Phys.* **36**, 260 (1964).

<sup>45</sup> R. E. Love, R. W. Shaw, and W. A. Fate, *Phys. Rev.* **138**, A1453 (1965).

<sup>46</sup> B. R. Tittmann and H. E. Bömmel, *Phys. Rev. Letters* **14**, 296 (1965).

<sup>47</sup> M. Levy and I. Rudnick, *Phys. Rev.* **132**, 1073 (1963).

<sup>48</sup> R. Weber, *Phys. Rev.* **133**, A1487 (1964).

<sup>49</sup> A. Granato and K. Lücke, *J. Appl. Phys.* **27**, 583 (1956).

<sup>50</sup> A. Granato and K. Lücke, *J. Appl. Phys.* **27**, 789 (1956).

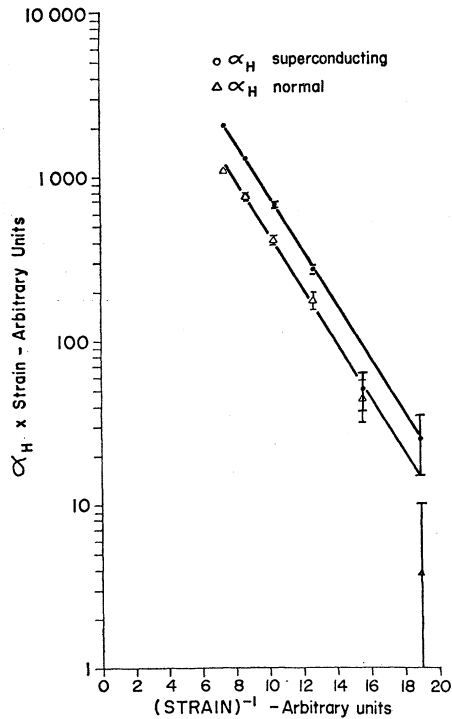


FIG. 10. Granato-Lücke plot (see Refs. 49 and 50) of the strain-amplitude dependent part of the attenuation in the normal and superconducting states.  $q \parallel [10\bar{1}0]$ ,  $s \parallel [0001]$ ,  $\omega = 58.1$  Mc/sec.

pinning points, coalesce, and get pinned at the dislocation network nodes. This growth of the dislocation line length requires energy which appears as attenuation,  $\alpha_H$ . Granato and Lücke's derivation yields,

$$\alpha_H = \frac{J_1(L_n)^3}{e(L_c)^2} \exp\left(-\frac{J_2}{eL_c}\right), \quad (17)$$

where  $J_1$  and  $J_2$  are constants that depend on the particular material investigated, and  $e$  is the strain amplitude.

Tittmann and Bömmel argue that at liquid-He temperatures normal electrons act as a viscous medium. This medium prevents the strain induced dislocations from gaining enough amplitude to break away from the impurity pinning points. In the superconducting state the electron's viscosity is supposedly lost and the Granato-Lücke mechanism enters into play. Tittmann and Bömmel have made several tests to verify the applicability of Eq. (17) to their data. This equation has no frequency dependence of  $\alpha_H$ , and they have found none. Equation (17) predicts a reduction of  $\alpha_H$  corresponding to a reduction in  $L_c$ . Tittmann and Bömmel verified this by adding impurities to their samples. A plot of  $\log(e\alpha_H)$  versus  $1/e$  for their data yields a straight line, as predicted by Eq. (17).

Figure 10 shows plots of  $\log(e\alpha_H)$  versus  $1/e$  for our

experiment. The value of  $\alpha_H$  is the difference between the attenuation at a given voltage and the attenuation below 50 V, where we assume  $\alpha_H = 0$ . The curves obtained for both the normal and the superconducting cases are seen to be straight lines, thus agreeing with the Granato-Lücke equation. The two lines can be drawn parallel to each other, and this implies that  $L_c$  is the same in both cases, as is to be expected. The two curves are separated by a constant factor of 1.8. If the Granato-Lücke equation is to be applied here as well, this factor implies that  $L_{ns}/L_{nn} = (1.8)^{1/3} = 1.2$ . However, it is difficult to see how the passage from the normal to the superconducting state can lead to a change in  $L_n$ , nor does Tittmann and Bömmel's viscous damping mechanism seem to be adaptable to our data.

## VI. SUMMARY OF RESULTS AND CONCLUSIONS

The principal results of our ultrasonic studies in thallium are as follows:

(1) Pippard's equation for the ultrasonic attenuation due to normal electrons has been verified for the case when the electrons' mean free path is smaller than the sound wavelength. In particular, the predicted direct dependence of attenuation on the sound frequency squared and inverse dependence on the sound velocity cubed have been found to hold. It has also been found that the free-electron Fermi surface yields a good approximation when used in Pippard's equation. The multiband structure of Tl affects the ultrasonic attenuation through the sound velocity term rather than through the explicit integration over the Fermi surface.

(2) The adiabatic elastic constants of Tl have been measured at 4.2 and 297°K. With these the Debye temperature and compressibilities of Tl are calculated; the resulting values agree with those found by others.

(3) The superconducting energy gap measured with shear waves is found to be anisotropic in Tl. Tl is the first superconductor in which a gap anisotropy appears when measurements are made with ultrasonic waves in which  $ql < 1$ . It would be of interest to measure the gaps in Tl under conditions such that  $ql \gg 1$  and down to temperatures where  $T/T_c \approx 0.1$ . These experiments would establish more firmly the existence of the gap anisotropy, and the presence of a discontinuous drop of shear wave attenuation at  $T_c$ . Furthermore such experiments would allow comparison with the Pokrovskii<sup>51</sup> and Privorotskii<sup>52</sup> calculations for the gap anisotropy for  $ql \gg 1$  and for small reduced temperatures.

*Note added in proof.* We have recently ascertained that the thallium, as received, contains an appreciable amount of sulfur.

<sup>51</sup> V. L. Pokrovskii, Zh. Eksperim. i Teor. Fiz. **40**, 898 (1961) [English transl.: Soviet Phys.—JETP **13**, 628 (1961)].

<sup>52</sup> I. A. Privorotskii, Zh. Eksperim. i Teor. Fiz. **42**, 450 (1962) [English transl.: Soviet Phys.—JETP **15**, 315 (1962)].